J. Cell. Mol. Med. Vol 13, No 9B, 2009 pp. 3303-3314

Formation of lipid raft redox signalling platforms in glomerular endothelial cells: an early event of homocysteine-induced glomerular injury

Fan Yi, Si Jin, Fan Zhang, Min Xia, Jun-Xiang Bao, Junjun Hu, Justin L. Poklis, Pin-Lan Li *

Department of Pharmacology & Toxicology, Medical College of Virginia Campus, Virginia Commonwealth University, VA, USA

Received: November 17, 2008; Accepted: February 22, 2009

Abstract

The present study tested the hypothesis that homocysteine (Hcys)-induced ceramide production stimulates lipid rafts (LRs) clustering on the membrane of glomerular endothelial cells (GECs) to form redox signalling platforms by aggregation and activation of NADPH oxidase subunits and thereby enhances superoxide ($O_2^{\cdot -}$) production, leading to glomerular endothelial dysfunction and ultimate injury or sclerosis. Using confocal microscopy, we first demonstrated a co-localization of LR clusters with NADPH oxidase subunits, $gp91^{phox}$ and $p47^{phox}$ in the GECs membrane upon Hcys stimulation. Immunoblot analysis of floated detergent-resistant membrane fractions found that in LR fractions NADPH oxidase subunits $gp91^{phox}$ and $p47^{phox}$ are enriched and that the activity of this enzyme dramatically increased. We also examined the effect of elevated Hcys on the cell monolayer permeability in GECs. It was found that Hcys significantly increased GEC permeability, which was blocked by inhibition of LR redox signalling platform formation. Finally, we found that Hcys-induced enhancement of GEC permeability is associated with the regulation of microtubule stability through these LR-redox platforms. It is concluded that the early injurious effect of Hcys on the glomerular endothelium is associated with the formation of redox signalling platforms *via* LR clustering, which may lead to increases in glomerular permeability by disruption of microtubule network in GECs.

Keywords: lipid microdomains • hyperhomocysteinemia • glomerular sclerosis • hyperfiltration

Introduction

Hyperhomocysteinemia (hHcys) is known as a critical pathogenic factor in the progression of end stage renal disease (ESRD) and in the development of cardiovascular complications related to ESRD [1–5]. We and others have demonstrated that oxidative stress mediated by NADPH oxidase is importantly involved in progressive glomerular injury or glomerulosclerosis associated with hHcys [6–8]. Although these results have indicated that activation of ceramide/NADPH oxidase signalling pathway contributes to homocysteine (Hcys) increased-superoxide ($O_2^{\cdot -}$) production in glomeruli [7, 8], it remains unknown how this ceramide-mediated signalling pathway is activated at an early stage of hHcys and thereby stimulates NADPH oxidase activity and produces local oxidative stress, ultimately leading to glomerular injury.

It is well known that the glomerulus consists of three major different cell components including endothelial, mesangial and epithelial cells such as podocytes, which constitute filtration membrane in glomeruli and determine glomerular filtration [9–12]. Among them, the glomerular capillary endothelium should be the first target tissue in the kidney during hHcys, and therefore the injury or dysfunction of glomerular capillary endothelial cells (GECs) may represent an early event in the development of glomerular injury induced by this injury factor. Indeed, there is considerable evidence that GEC damage under conditions of haemolytic uremic syndrome, preeclampsia, diabetes and hypertension with the onset of microalbuminuria plays an important role in the development of glomerular sclerosis and ESRD [13, 14]. Recently, many studies have re-emphasized the pathogenic role of injured GECs in progression of glomerulosclerosis or ESRD [10]. In this regard, it has been reported that

*Correspondence to: Pin-Lan LI, M.D, Ph.D.,
Department of Pharmacology and Toxicology,
Medical College of Virginia, Virginia, Commonwealth University,
410 N 12th, Richmond, VA 23298, USA.
Tel.: (804) 828-4793
Fax: (804) 828-4794
E-mail: pli@vcu.edu

doi:10.1111/j.1582-4934.2009.00743.x

© 2009 The Authors
Journal compilation © 2009 Foundation for Cellular and Molecular Medicine/Blackwell Publishing Ltd

endothelial cell injury immediately leads to an increase in glomerular capillary permeability and thereby enhances flux of blood components such as albumin out of glomerular capillaries, which inevitably causes mesangial cell injury, reactive mesangial proliferation and excessive production of extracellular matrix, resulting in the progression of glomerular injury or sclerosis [10]. Therefore, increased glomerular endothelial permeability is considered as an important early hallmark of pathological conditions in ESRD. To our knowledge, it remains unknown whether or how increased plasma Hcys damages GECs and thereby increases glomerular permeability, thereby resulting in glomerular injury or sclerosis.

Given evidence that Hcys induces ceramide synthesis and ceramide may promote cell membrane lipid rafts (LRs) clustering and thereby aggregate many signalling molecules to form LR redox signalling platforms in endothelial cells, mediate transmembrane signalling [15–17], we suggested that Hcys-induced ceramide production may stimulate LR clustering on the membrane of GECs to form redox signalling platforms by aggregation and activation of NADPH oxidase subunits and enhances $O_2^{\cdot -}$ production, thereby leading to GEC dysfunction and ultimate glomerular injury.

To test this hypothesis, we first determined whether Hcys stimulates LR clustering to form redox signalling platforms by aggregation and activation of NADPH oxidase subunits in GECs using confocal microscopy and membrane fraction floatation. We also determined the contribution of this LR redox signalling platform formation to endothelial dysfunction associated with Hcys by examining their actions on the permeability of GECs layer preparations. Then, we went on to determine whether Hcys-induced LR redox signalling platform formation is associated with the regulation of microtubule network stability, a critical factor for the maintenance of endothelial barrier function. Our results demonstrate that Hcys induces the formation of LR redox signalling platforms in GECs, which contributes to Hcys-enhanced endothelial cell permeability by disruption of microtubule network.

Materials and methods

Cell culture

GECs were isolated and cloned as reported previously [18, 19]. GEC colony used in the present study was a kindly gift from Dr. Masaomi Nangaku, University of Tokyo School of Medicine and Dr. Stephen Adler, New York Medical College. These cells were isolated from glomeruli of male Sprague-Dawley rats and cultured and their characteristics are kept such as positive staining with JG12, but negative labelling of podocalyxin, nephrin, α-smooth muscle actin and ED-1. These cells were maintained in RPMI 1640 containing 2000 mg/L glucose, supplemented with 10% foetal bovine serum (FBS) (JRH Biosciences, Lenexa, KS, USA) and 10% NuSerum (BD Biosciences, Bedford, MA, USA) at 37°C under a humidified atmosphere of 5% CO_2/95% air for use.

Liquid chromatography–electrospray ionization tandem mass spectrometry (LC-ESI-MS-MS) for quantitation of ceramide

Separation, identification and quantitation of ceramide in GECs were performed by LC/MS. The HPLC equipped with a binary pump, a vacuum degasser, a thermostated column compartment and an autosampler (Waters, Milford, MA, USA). The HPLC separations were performed at 70°C on a RP C18 Nucleosil AB column (5 μm, 70 mm $\times$ 2 mm i.d.) from Macherey Nagel (D¸ren, Germany). The mobile phase was a gradient mixture formed as described [20]. The cell lipids were extracted according to previous studies [7]. To avoid any loss of lipids, the whole procedure was performed in siliconized glassware. MS detection was carried out using a Quattro II quadrupole mass spectrometer (Micromass, Altrincham, England) operating under MassLynx 3.5 and configured with a Z-spray electrospray ionization source. Source conditions were described as previously [20].

Confocal microscopy of LR clusters and its co-localization with NADPH oxidase subunits in GECs

For confocal microscopic detection of LR platforms or LR-associated proteins, GECs were grown on poly-L-lysine-coated glass cover slips and then treated with Hcys (50–200 μM, 30 min.) to induce LR clustering. In additional group of cells, the LR disruptors, nystatin (10 μg/ml, Sigma, St. Louis, MO, USA) and methyl-β-cyclodextrin (MCD, 1 mM, Sigma) were added to pretreat cells for 20 min. before Hcys stimulation.

Detection of LR clusters were performed as we described previously [21–23]. In brief, G_{M1} gangliosides enriched in LRs were stained with FITC-labelled cholera toxin (CTX; 1 μg/ml, 30 min., Molecular Probes, Carlsbad, CA, USA). The patch formation of FITC-labelled CTX and gangliosides complex represented the clusters of LRs. Clustering was defined as one or several intense spots of fluorescence on the cell surface, whereas unstimulated cells displayed a homogenous distribution of fluorescence throughout the membrane. In each experiment, the presence or absence of clustering in samples of 200 cells was scored by two independent observers. The results are given as the percentage of cells showing a cluster after the indicated treatment as described. For dual staining detection of the co-localization of LRs and ceramide or NADPH oxidase subunits anti-gp91^{phox}, anti-p47^{phox}, GECs were incubated for 1 hr at room temperature with indicated primary monoclonal mouse anti-ceramide (1 : 100, Sigma), anti-gp91^{phox} or anti-p47^{phox} (1 : 100, BD biosciences, San Jose, CA USA) followed by incubation with 5 μg/ml Texas red-conjugated antimouse antibody for an additional 2 hrs at room temperature. FITC-CTX staining was then performed as described above. Negative control staining was performed with irrelevant monoclonal antibodies.

Isolation of LR membrane fractions from GECs by gradient centrifugation

LR fractions were isolated as we described previously [22]. GECs were lysed in 1.5 ml MBS buffer containing (in μM): morpholinoethane sulfonic acid, 25; NaCl, 150; ethylenediaminetetraacetic acid, 1; PMSF, 1; Na_3VO_4, 1; and a mixture of 'complete' protease inhibitors (Roche, Nutley, NJ, USA)

© 2009 The Authors
Journal compilation © 2009 Foundation for Cellular and Molecular Medicine/Blackwell Publishing Ltd

and 2% Triton X-100 (pH 6.5). Cell extracts were further homogenized by 10 passages through a 25-gauge needle, and then homogenates were adjusted with 60% OptiPrep Density Gradient medium (Sigma) to 40% and overlaid with equal volume (4.5 ml) of discontinuous 30% to 5% OptiPrep Density Gradient medium. Samples were centrifuged at 32,000 rpm for 30 hrs at 4°C using a SW32.1 rotor (Beckman, Fullerton, CA, USA). Thirteen fractions were collected from the top to the bottom (fraction numbers 1 to 13), which were ready for immunoblot analysis.

Immunoprecipitation and immunoblotting analysis

The homogenates, cytosol, or membrane of GECs were prepared as we reported previously [24]. In brief, 20 μg proteins or 50 μl of resuspended proteins (for immunodetection of LR-associated proteins) were subjected to SDS-PAGE, transferred onto a nitrocellulose membrane and blocked as described previously. The membrane was probed with primary antibodies anti-flotillin-1, anti-gp91^{phox}, anti-p47^{phox}, anti-p67^{phox} (1 : 1000, BD Biosciences), anti-p22^{phox} (1 : 500 dilution, Santa Cruz Biotech, Santa Cruz, CA, USA) and anti-Rac (1 : 1000 dilution, Upstate, Lake Placid, NY, USA) overnight at 4°C followed by incubation with horseradish peroxidase-labelled antimouse overnight at 4°C followed by incubation with horseradish peroxidase-labelled antimouse IgG or anti-rabbit IgG (1 : 5000, Sigma). The immunoreactive bands were detected by chemiluminescence methods (Pierce, Rockford, IL, USA) and visualized on Kodak Omat film.

Immunoprecipitation followed by immunoblotting analysis was performed to detect the phosphorylation status of p47^{phox} as described by previous studies [25]. Immunoprecipitation was performed by incubating cell lysate with goat polyclonal anti-p47^{phox} (Upstate) for 2 hrs, followed by precipitation with agarose-immobilized protein A. The immunoprecipitated proteins were then subjected to Western blot analysis using a mouse monoclonal anti-phosphoserine antibody (R & D system, Minneapolis, MN, USA). The protein levels of p47^{phox} in the immunoprecipitates were also determined by Western blot analysis using goat polyclonal anti-p47^{phox} antibody. Phosphorylated p47^{phox} protein levels were normalized to the total p47^{phox} detected in the immunoprecipitates.

Detection of $O_2^{\cdot -}$ production in intact GECs and LR fractions

Dynamic changes in $O_2^{\cdot -}$ production in intact GECs were determined by fluorescent microscopic imaging of single cells as we described previously [26]. This method is based on the DNA binding characteristic of oxidized dihydroethidium product ethidium within cells when they were stimulated by Hcys. To further confirm Hcys-induced NADPH oxidase activity in LR fractions, $O_2^{\cdot -}$ production in both LR fractions and non-raft fractions was measured by electromagnetic spin resonance (ESR). $O_2^{\cdot -}$ production was normalized by protein concentration and detailed procedures were described in our previous studies [22].

Cell permeability assay

The permeability of GECs layer was measured according to the methods described as previous studies [27, 28]. Briefly, GECs were seeded in the upper chambers of 0.4 μm polycarbonate Transwell filters of a 24-well filtration microplate (Whatman Inc., Florham Park, NJ, USA). After reaching confluence, the culture medium was replaced with fresh phenol red-free RPMI 1640 in the presence of Hcys and 70 kD FITC-dextran (2.5 μmol/l) in the upper chambers. After Hcys-treatment for 4–24 hrs, the filtration microplate was removed and the medium from the lower compartment was collected, then fluorescence was measured in a spectrofluorimeter at 494 nm excitation and 521 nm emission. The relative permeable fluorescence intensity was indicated as relative cell permeability.

Immunofluorescent microscopic analysis of GEC microtubule network

For microtubule network analyses, GECs were treated with Hcys and related LR disruptor and inhibitors, washed with phosphate-buffered saline (PBS; pH = 7.2), and then fixed. Then, these cells were stained with anti-β-tubulin antibody (1 : 100; Abcam, Cambridge, MA, USA) after blocking with 1% bovine serum albumin (Sigma) in PBS for 30 min at room temperature, which was followed by washing cells four times with PBS. Finally, FITC-labelled secondary antibody was added and cells were embedded into gelatine solution. Microtubule staining was analysed using a Nikon ECLIPSE E 800 fluorescence microscope attached to a digital imaging system (Nikon, Tokyo, Japan). Quantitative analysis of assembled microtubule was performed with MetaVue 4.6 (Universal Imaging, Downington, PA, USA). To assess microtubule assembly or network, individual GECs were outlined first and then images were differentially segmented between cytosol (black) and microtubules (highest grey value) based on image greyscale levels. The ratio of the area covered by microtubule within cells to the whole cell was determined [29].

Data analysis

Data are presented as mean ± S.E. Significant differences between and within multiple groups were examined using ANOVA for repeated measures, followed by a Duncan's multiple-range test. Student's t-test was used to evaluate the significant differences between two groups of observations. $P < 0.05$ was considered statistically significant.

Results

Quantitation of ceramide levels in Hcys-treated GECs

Previous studies in our laboratory have demonstrated LR clustering trigged by ceramide occurs in coronary endothelial cells to form the redox signalling platform on the cell membrane, which mediates NADPH oxidase activation, resulting in increased $O_2^{\cdot -}$ production endothelial dysfunction. However, it remains unknown whether Hcys increases ceramide production in GECs and initiates the formation of redox signalling platforms. Using LC/MS analysis, we identified and quantified seven different major ceramides (C14, C16, C17, C18, C20, C22 and C24) in GECs with or without Hcys stimulation. Among them, C24 ceramide is the most

© 2009 The Authors
Journal compilation © 2009 Foundation for Cellular and Molecular Medicine/Blackwell Publishing Ltd

abundant species. As summarized data in Table 1, Hcys significantly increased total ceramide levels by 40.2%.

No effect of Hcys on NADPH oxidase expression level

Our preliminary results indicated that Hcys enhanced $O_2^{\cdot -}$ production in GECs, to determine whether increased NADPH oxidase-mediated $O_2^{\cdot -}$ production is associated with an increase in the protein levels of NADPH oxidase, Western blot analysis was performed. It was found that there was no change in the protein levels of NADPH oxidase subunits including $p47^{phox}$, $p67^{phox}$, $p22^{phox}$, $gp91^{phox}$ and Rac in Hcy-treated GECs (Fig. 1A). These results indicated that activation of NADPH oxidase in Hcy-treated cells was not due to an increase in enzyme protein levels.

Phosphorylation of $p47^{phox}$ and translocation of $p47^{phox}$ into cell membrane

To further investigate the mechanism by which Hcy treatment activated NADPH oxidase-dependent $O_2^{\cdot -}$ production, the phosphorylation status of $p47^{phox}$ was examined. By immunoprecipitation and immunoblotting analyses, we found that there was a significant increase in serine phosphorylation of $p47^{phox}$ in Hcy-treated GECs with time-dependent manner (Fig. 1B). The levels of $p47^{phox}$ were also found to be increased in the membrane fraction of Hcy-treated cells as compared with control cells (Fig. 1C and D). These results indicated that Hcys-induced NADPH oxidase activation in GECs is associated with increased phosphorylation and subsequent membrane translocation of $p47^{phox}$.

LR clustering and aggregation or recruitment of redox signalling molecules in the membrane of Hcys-treated GECs

Previous studies have shown that increased ceramide production results in LR clustering in endothelial cells [21] and therefore we examined whether Hcys also induces LR clustering due to its action on ceramide production. In these experiments, GECs were treated with Hcys and stained with FITC-CTX, and then the distribution of FITC-CTX (as LR marker) labelled LR patches was visualized on the cell membrane. As shown in Fig. 2A, in control cells, LRs were evenly spread throughout the cell membrane under control condition as indicated by weak diffuse green FITC fluorescence. Upon stimulation with Hcys, these LRs in the membrane of GECs formed multiple platforms as displayed by large and intense green fluorescence patches. The right panel of Fig. 2A summarized the effects of Hcys on LR clustering in cell membranes by counting these LR patches. In GECs, there were 15.2% of the cells displayed with intense LR clusters under resting condition, while

Table 1 Ceramide concentrations in Hcys-treated GECs (nmol/mg protein) measured by LC/MS spectrometry

Ceramide	Control	Hcys treated
C16	0.1967 ± 0.016	0.3109 ± 0.092*
C17	0.0075 ± 0.003	0.0098 ± 0.003*
C18	0.0258 ± 0.006	0.0279 ± 0.007
C20	0.01974 ± 0.011	0.0298 ± 0.012*
C22	0.1701 ± 0.0310	0.1853 ± 0.030
C24	0.7267 ± 0.1138	1.0423 ± 0.113*
Total	1.1466 ± 0.1550	1.606 ± 0.1295*

*$P < 0.05$ versus control, n = 5

52% of the cells showed clustering of LR after stimulation with Hcys. This Hcys-induced LR clustering was substantially blocked by nystatin and MCD, two well-known disruptors of LRs.

Furthermore, GECs were stained by an FITC-labelled CTX and an anti-ceramide antibody labelled with Texas red. Under control conditions, both FITC and Texas red staining was diffuse and their co-localization in overlaid images was in diffuse or small yellow dots. When the cells were stimulated by Hcys, a number of large patches or spots with co-localization of both components (yellow in overlaid image) on the cell membrane were detected.

To examine whether NADPH oxidase subunits are able to aggregate or cytosolic subunits such as $p47^{phox}$ after phosphorylation, specific tanslocate into LR fractions to form a redox signalling platform on the cell membrane, we stained GECs with both Texas red-conjugated anti-$p47^{phox}$ and FITC-CTX, and the distribution of anti-$p47^{phox}$ within LRs clusters was visualized in the GEC membrane by confocal microscopy. As shown in Fig. 2C, $p47^{phox}$ evenly spread throughout the whole cell including membrane and cytosolic parts under normal condition. When GECs were treated with Hcys, $p47^{phox}$ translocated to membrane as shown by red fluorescence spot or patches. When two sequentially scanned images from the same cell with different wavelengths (for FITC and Texas red) were merged together, there were a number of yellow areas either as dots or as patches resulted from green CTX and Texas red-antibody (right images). These yellow patches were considered as a co-localization of LR components and $p47^{phox}$. These results indicated that this translocation of $p47^{phox}$ into cell membrane, specific located in LR fraction. In addition, similar co-localization results were obtained when GECs were stained with Texas red-conjugated anti-$gp91^{phox}$ and FITC-CTX (data not shown). These results indicated that these LR clusters with recruitment or aggregation of NADPH oxidase subunits formed a number of LR-NADPH oxidase complexes, now these LR-NADPH oxidase clusters or complexes that possess redox signalling function have been referred to as membrane LR redox signalling platforms.

There was a concern over the specificity of such Hcys-induced LR redox signalling platforms to the kidney cells. To address this

© 2009 The Authors
Journal compilation © 2009 Foundation for Cellular and Molecular Medicine/Blackwell Publishing Ltd

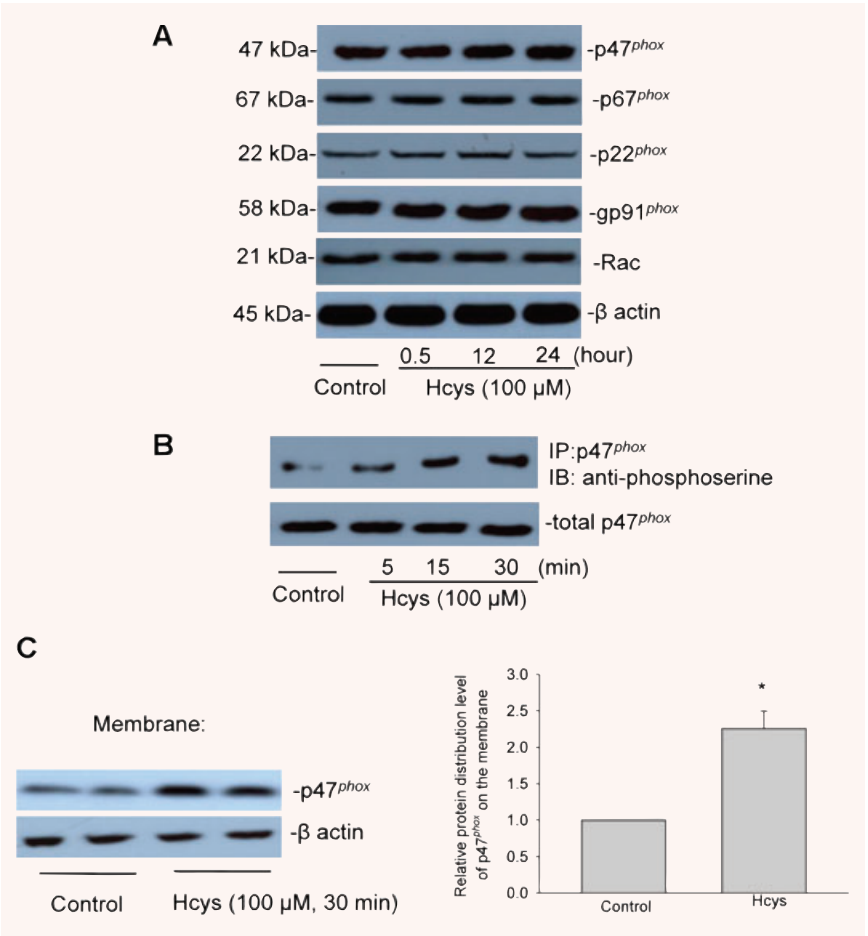

Fig. 1 Effects of Hcys on NADPH oxidase subunit protein levels, phosphorylation of $p47^{phox}$ and the translocation of $p47^{phox}$ in GECs. (**A**) Immunoblot for NADPH oxidase subunits including $p47^{phox}$, $p67^{phox}$, $p22^{phox}$, $gp91^{phox}$ and Rac in the homogenates of GECs with or without treatment of Hcys for various time periods. (**B**) Phosphorylation of $p47^{phox}$ subunits at different time treatments. Cells were incubated with Hcys (100 μM) or without Hcys for various time periods. $p47^{phox}$ were immunoprecipitated using anti-$p47^{phox}$ antibody followed by Western blot analysis (IB) using anti-phosphoserine antibody to detect serine-phosphorylated proteins. The immunoblots were analysed by densitometry. (**C**) Cells were incubated for 30 min in the absence (control) or presence of Hcy (100 μM). The membrane fraction was prepared for detection of $p47^{phox}$ protein by Western blot analysis. Representative blots (upper) and summarized results indicating the relative protein level of $p47^{phox}$ protein in the membrane fraction. $^{*}P < 0.05$ *versus* control ($n = 5$).

issue, we compared the effect of Hcys on the LR redox signalling platform formation with that in other endothelial cells such as bovine coronary arterials endothelial cells (BCAECs). These additional experiments showed that, similar to GECs, Hcys induced LR clustering in BCAECs. Furthermore, co-localization results were also obtained when GECs were stained with Texas red-conjugated anti-$p47^{phox}$ and FITC-CTX as shown in Fig. 2D, suggesting that LR redox platform formation may be a general phenomenon during Hcys treatment.

Enrichment of both $p47^{phox}$ and $gp91^{phox}$ in LR fractions

To further confirm the LR redox signalling platform formation, LR fractions were isolated by membrane flotation and related proteins were probed in these LR fractions. As shown in Fig. 3A, Western blot analysis showed a positive expression of flotillin-1 in fractions 5 to 6 (from top to bottom), which were referred to LR fractions. NADPH oxidase subunits, $gp91^{phox}$ could be detected in most of the membrane fractions from GECs; however, there was a distribution change among these fractions with a marked increase in $gp91^{phox}$ protein in LR fractions when GECs were stimulated by Hcys. This Hcys-induced increase in $gp91^{phox}$ in LR fractions was significantly inhibited by pre-treatment of GECs with MCD. Similarly, $p47^{phox}$ was also found significantly increased in LR fractions upon Hcys stimulation, which was also inhibited by MCD. The summarized results were shown in Fig. 3B. Another LR disruptor, nystatin, also blocked Hcys-induced enrichment of both NADPH oxidase subunits in LR fractions (data not shown).

Inhibition of Hcys-enhanced NADPH oxidase activity by disruption of LR clustering

Using high-speed wavelength-switching technique, we simultaneously monitored the fluorescence intensity of ethidium-DNA complex within GECs. It was found that Hcys enhanced $O_2^{\cdot-}$ production by more than two folds, which was blocked by LR disruption and inhibition of NADPH oxidase. Summarized results are presented

© 2009 The Authors
Journal compilation © 2009 Foundation for Cellular and Molecular Medicine/Blackwell Publishing Ltd

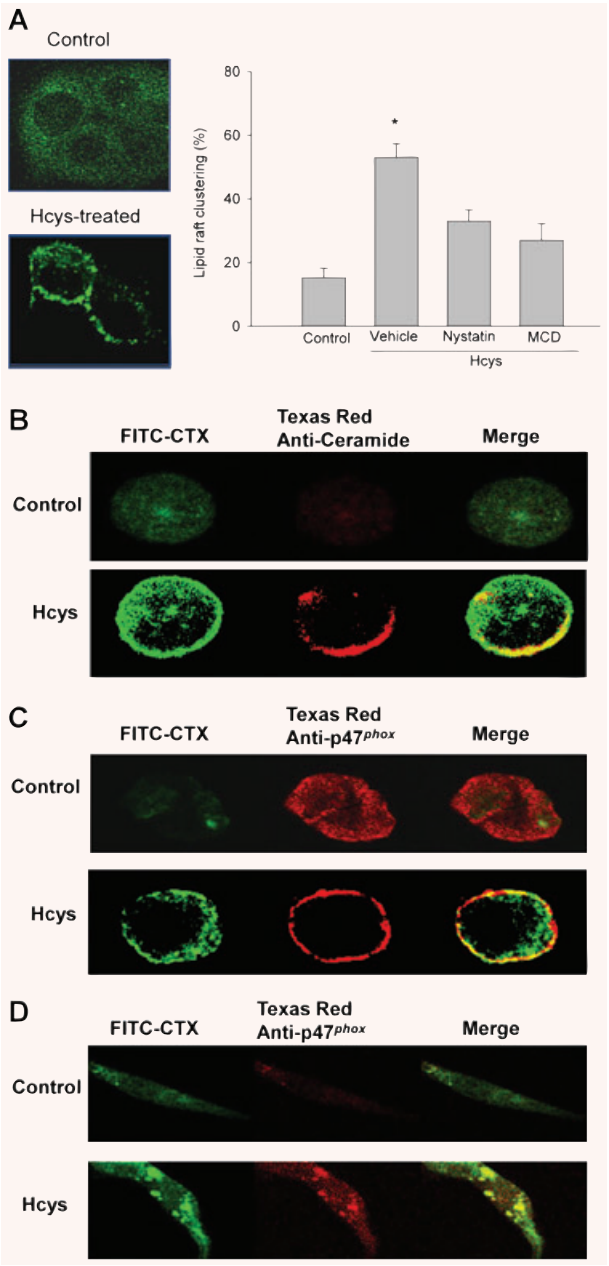

Fig. 2 LR clustering and aggregation or recruitment of signalling molecules in the membrane of ECs by confocal microscopic analysis. (**A**) Representative confocal microscopic images show the different extent of LR clustering on the membrane of unstimulated (control) or stimulated GECs (Hcys). Summarized data on the right panel showing the effect of LR disruptors on the formation of LRs clusters. Panel bars displays mean values ± S.D. of five experiments with analysis of more than 1000 GECs. (**B**) Representative confocal microscopic images of LR clusters in GECs. FITC-CTX was shown as a pseudo green colour on the left; Texas red-conjugated anti-ceramide shown as red colour in the middle; and overlaid images shown on the right. Yellow spots or patches in overlaid images were defined as LRs clusters. (**C**) Confocal microscopic images of LRs in GECs (FITC-CTX green fluorescence on the left), $p47^{phox}$ (Texas red-conjugated anti-$p47^{phox}$ in the middle) and overlaid images (right). Yellow areas of overlaid images represent co-localization of $p47^{phox}$ and CTX-labelled G_{M1} gangliosides. (**D**) Confocal microscopic images of LRs in BCAECs (FITC-CTX green fluorescence on the left), $p47^{phox}$ (Texas red-conjugated anti-$p47^{phox}$ in the middle) and overlaid images (right). Yellow areas of overlaid images represent co-localization of $p47^{phox}$ and CTX-labelled G_{M1} gangliosides. $^{*}P < 0.05$ *versus* control ($n = 5$).

in Fig. 4A, and a time-dependent increase in $O_2^{\cdot -}$ production was observed when Hcys was added to stimulate cells. In the presence of LR disruptors or NADPH oxidase inhibitor (Apo, 100 μM), Hcys-induced $O_2^{\cdot -}$ production was substantially blocked.

We also analysed NADPH oxidase activity by measurement of $O_2^{\cdot -}$ production in both isolated LR-enriched and non-raft fractions using ESR. As shown in Fig. 4B, we found that Hcys at least doubled $O_2^{\cdot -}$ production in LR fraction, which was inhibited by nystatin, MCD and Apo. In non-LR fraction, only a 36% increase in $O_2^{\cdot -}$ production during Hcys stimulation was observed.

Blockade of Hcys-induced GEC monolayer permeability by disruption of LR clustering

To determine the role of LR clustering in mediating Hcys-induced GEC dysfunction, we examined its effect on the permeability of GEC monolayers to FITC-dextran. The possible effects of Hcys and cysteine on the GEC permeability were examined. Hcys was tested at 100 μM which was demonstrated to generate maximal action to increase ceramide production, activate NADPH oxidase and induce glomerular injury and cysteine as control. After a 16-hr treatment, there was no significant increase in GEC permeability with cysteine, while Hcys induced a significant increase in GEC permeability in a time dependent manner (Fig. 5A). This Hcys-induced increase permeability was markedly reduced by pre-treatment with NADPH oxidase inhibitor Apo or LR disruption compounds nystatin and MCD as summarized in Fig. 5B. Compared to control, there was no significant difference when GECs were treated these inhibitors alone.

Involvement of microtubule network in Hcys-induced GEC permeability

To assess the state of microtubule network in Hcys-challenged GECs, we performed immunofluorescent microscopy utilizing anti-β-tubulin antibody. It was found that there were significant morphological changes in microtubule network appearance upon Hcys stimulation, which was Hcys concentration dependent as shown in Fig. 6A. Compared to control GECs, moderate microtubule rearrangement and microtubule depolymerization were shown at low concentrations of Hcys (50 μM) and when higher

© 2009 The Authors
Journal compilation © 2009 Foundation for Cellular and Molecular Medicine/Blackwell Publishing Ltd

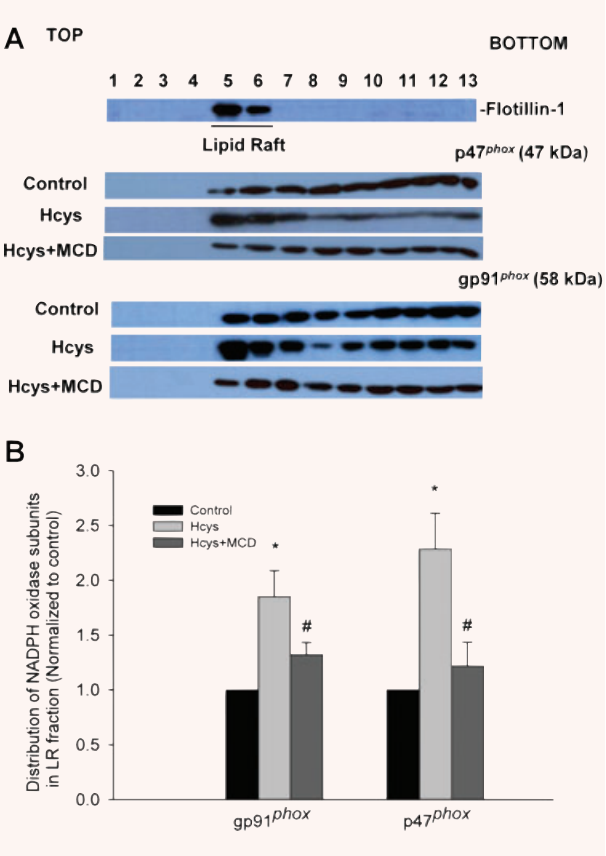

Fig. 3 Distribution and localization of $p47^{phox}$ and $gp91^{phox}$ in floated membrane fractions from GECs. (**A**) Typical gel documents of Western blot analysis showing distribution and localization of $gp91^{phox}$ and $p47^{phox}$ in LR and non-raft membrane fractions from GECs. Numbers on the top indicate membrane fractions isolated by gradient centrifugation from top to bottom. (**B**) Summarized data depicting the enrichment of NADPH oxidase subunits $gp91^{phox}$ and $p47^{phox}$ in LR fractions for GECs. $^{*}P < 0.05$ *versus* control; $^{\#}P < 0.05$ *versus* Hcys ($n = 5$).

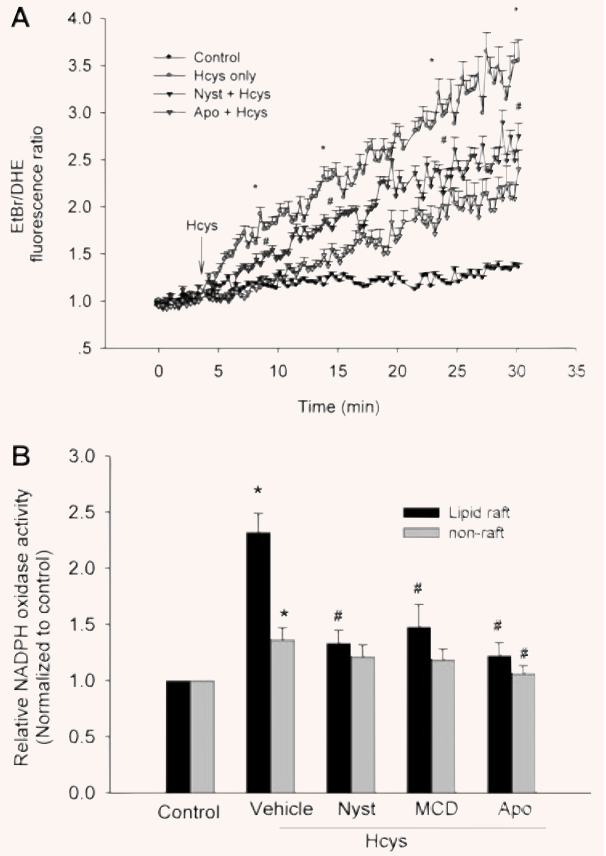

Fig. 4 Effects of LR disruption on Hcys-induced increase in NADPH oxidase activity in intact GECs and LR fractions. (**A**) Time-dependent conversion of dihydroethidium into Eth-DNA for measurement of $O_2^{\cdot -}$ level by fluorescent microscopic imaging analysis in intact GECs under control condition and with Hcys stimulation before and after inhibition of NADPH oxidase. (**B**) Summarized data depicting the effects of LR disruption on Hcys-induced increase in NADPH oxidase activity in LR- and non-raft fractions. $^{*}P < 0.05$ *versus* control; $^{\#}P < 0.05$ *versus* Hcys ($n = 5$).

concentrations (100 and 200 μM) of Hcys were used, tubulins in microtubule network were significantly reduced and remaining microtubules appear disoriented and collapsed towards the centrosome area (Fig. 6A). However, cysteine had no significant effect of microtubule structure. TGF-β_1, a detriment factor to disrupt microtubule stability was used as a positive control [29]. In addition, similar changes with microtubule depolymerization and disruption were obtained when GECs were treated with xanthine/xanthine oxidase (X/XO), an exogenous $O_2^{\cdot -}$ generating system. This action of X/XO was blocked by SOD (300 U/ml), a $O_2^{\cdot -}$ dismutase, indicating Hcys-induced microtubule destabilization is associated with oxidative stress associated with LRs. Quantitative results from morphometric analysis are summarized in Fig. 6B, which used a ratio of assembled microtubule network *versus* total cell area to depict microtubule network area or stability in treated GECs during different stimuli.

Moreover, NADPH oxidase inhibitor Apo and LR disruptors, nystatin significantly attenuated Hcys-induced microtubule network destabilization and damage which was similar to the results obtained when GECs were treated by microtubule stabilizer taxol (10 nM) (Fig. 7A).

To further confirm whether Hcys-induced microtubule network disruption is associated with GEC permeability, we treated the GEC monolayer with taxol and measured its permeability. It was found that taxol improved Hcys-induced cell permeability which was consistent with results obtained during NADPH oxidase inhibition by Apo as described above. Summarized data are shown in Fig. 7B.

© 2009 The Authors
Journal compilation © 2009 Foundation for Cellular and Molecular Medicine/Blackwell Publishing Ltd

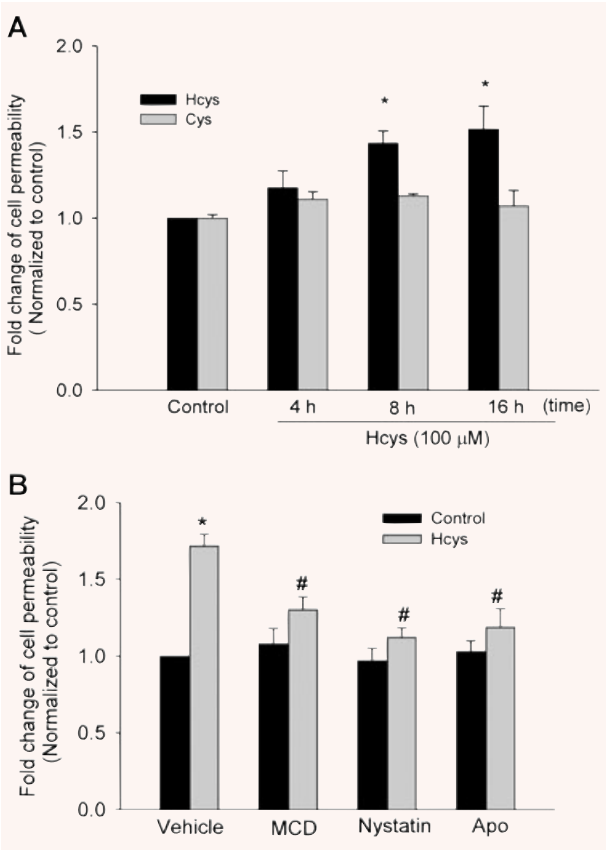

Fig. 5 Effect of Hcys on GEC permeability. (**A**) Summarized data showing Hcys-induced increases in GEC monolayer permeability in a time-dependent manner. (**B**) Effects of LR disruption and NADPH oxidase inhibition on Hcys-induced enhancement of GEC monolayer permeability. $^{*}P < 0.05$ *versus* control; $^{\#}P < 0.05$ *versus* Hcys ($n = 5$).

Discussion

There are considerable evidence that Hcys-induced endothelial dysfunction is an important pathogenic mechanism in the development of atherosclerosis and thrombosis [30, 31], and endothelial dysfunction or injury is considered as a critical initiating mechanism to cause different vascular or systemic diseases such as atherosclerosis, hypertension, diabetes and ESRD. However, how endothelial injury occurs at the early stage is still poorly understood. In recent studies, our laboratories have demonstrated that LR clustering to form redox signalling platforms importantly mediates the action of death receptor activation to induce endothelial dysfunction [22, 23, 32]. In this process, ceramide plays an essential role in initiating the formation of LR redox signalling platforms by formation of ceramide-enriched microdomains [15–17]. These ceramide-enriched microdomains can spontaneously fuse to form larger ceramide-enriched microdomains or platforms in response to death receptor activation, where NADPH oxidase subunits are assembled to produce redox molecules. It is well accepted that $p47^{phox}$ translocation is a key step, to some extent, a marker event, for the assembly and activation of NADPH oxidase since it is first translocated during the assembly process of these enzyme subunits. It has been reported that $p47^{phox}$ translocation is initiated by the phosphorylation of this subunit at various phosphorylation sites by PKC, PKA or MAPK. However, for a long time it is unknown how $p47^{phox}$ translocation and subsequent assembly of other NADPH oxidase subunits occur on the cell membrane. Given the role of ceramide in LR clustering to form LR platforms and the early and rapid response of LR platform formation to agonistic stimuli, it is possible that this LR platform formation is a major initiating mechanism this assembly or activation process of NADPH oxidase for Hcys-induced endothelial dysfunction. In the present study, we demonstrated that Hcys significantly enhanced ceramide production in GECs. By confocal microscopy, increased ceramide was found abundant in Hcys-induced LR platforms. It is possible that this increased ceramide in GECs may trigger LR clustering to form signalling platforms when these cells are exposed high level of Hcys, which initiate an early event of endothelial injury.

To test this hypothesis, we first confirmed that Hcys induced $p47^{phox}$ phosphorylation and consequent translocation to membrane. Then we detected whether this $p47^{phox}$ specifically translocate into LR fractions on the membrane with other subunits aggregation to form LR signalling platform. Using confocal microscopic analysis of LR marker, FITC-CTX and Texas red-conjugated $p47^{phox}$ or $gp91^{phox}$, we demonstrated that Hcys stimulated LR clustering and $p47^{phox}$ or $gp91^{phox}$ co-localized with LR, which was also confirmed by enhanced enrichment of NADPH oxidase subunits $p47^{phox}$ and $gp91^{phox}$ in LR fractions isolated by membrane floatation. These results provide evidence that NADPH oxidase subunits can be aggregated on or translocated into LR platforms (or ceramide-enriched microdomains) in response to Hcys challenge. This LR clustering may provide a driving force to promote the formation of NADPH oxidase-mediated redox platform, which may be a prerequisite to initiate assembling of other subunits and consequent activating cascade of this enzyme. To provide direct evidence that aggregation or assembling of NADPH oxidase components *via* LR clustering is involved in the activation of this enzyme, we directly determined NADPH oxidase-derived $O_2^{\cdot -}$ production in isolated LR fractions from GECs using ESR technique. It was found that Hcys indeed increased NADPH oxidase activity in these LR fractions, which was also blocked by its inhibitors and LR disruptors that were used to treat cells before preparation of LR membrane fraction. In addition, LR-clustering enhanced $O_2^{\cdot -}$ production was also found to be stimulated or boosted in intact single GECs as measured by fluorescent microscopic imaging analysis. The Hcys-induced increase of NADPH oxidase activity in intact GECs was substantially abolished by LR disruptors. These results suggest that aggregated NADPH oxidase subunits in LR platforms are functioning as an active enzyme complex. To further address whether the formation of LR

© 2009 The Authors
Journal compilation © 2009 Foundation for Cellular and Molecular Medicine/Blackwell Publishing Ltd

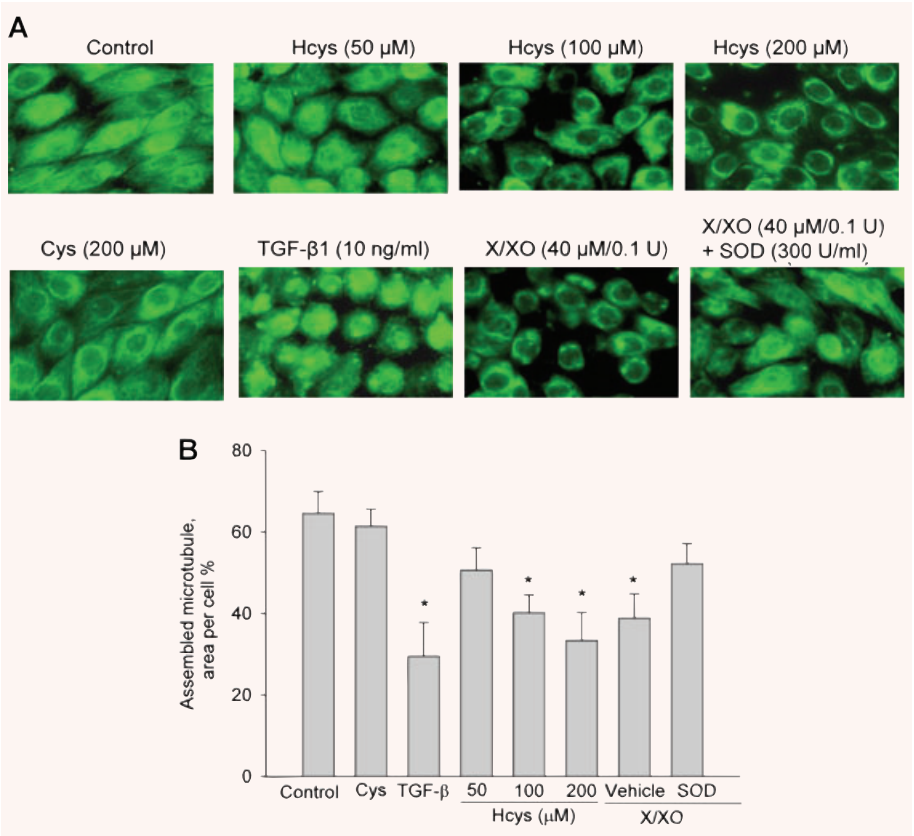

Fig. 6 Concentration-dependent effect of Hcys on microtubule network structure. (**A**) Representative images showing the effects of Hcys (50, 100, 150 and 200 μM), Cys (200 μM as thiol control), TGF-β_1 (10 ng/ml as positive control in disturbing microtubule structure) and X/XO (40 μM /0.1 U, a $O_2^{\cdot -}$ generating system) with or without SOD (300 U/ml) pre-treatment on microtubule network structure. (**B**) Morphometric data showing the microtubule derangement induced by Hcys before and after LR disruption. Data were expressed as percent of control (non-stimulated cells). Panel bars display the mean value ± S.D. of five experiments with analysis of more than 200 cells.

redox signalling platforms is ubiquitous during Hcys-mediated endothelial cell dysfunction, coronary endothelial cells were used as comparison. It was found that Hcys also induced LR redox signalling platforms formation in these endothelial cells. Taken together, our findings support the view that LRs clustering contributes to Hcys-induced activation of NADPH oxidase by aggregation and recruitment of its subunits to LR platforms in the cell membrane of ECs, which produces redox molecules to regulate downstream effectors' response and ultimately results in endothelial dysfunction.

To further explore the functional significance of LR redox signalling platforms in GECs, we determined the role of the formation of these LR redox signalling platforms in mediating Hcys-induced enhancement of GEC monolayer permeability. It is well known that the endothelium that regulates the passage of macromolecules and circulating cells from blood to tissues is a major target of oxidant stress and thereby endothelial dysfunction plays a critical role in the pathophysiology of many vascular and renal diseases [33, 34]. In regard to the regulation of vascular permeability, there is substantial evidence that oxidant stress increases vascular endothelial permeability [35, 36] and increased endothelial and ultimate glomerular permeability importantly contributes to the development of glomerular injury and sclerosis. However, there is no direct evidence so far concerning the effect of Hcys on GEC or glomerular permeability. The present study has shown that Hcys increased the permeability of GEC monolayer in a LR clustering-dependent manner. This LR clustering and consequent formation of redox signalling platforms may induce local oxidative stress and leads to increased permeability of GEC monolayer. The results for the first time link LR-mediated transmembrane signalling to glomerular permeability through redox mechanism. NADPH oxidase associated with LRs clustering plays an important role in mediating the effects of Hcys on GEC permeability.

It is well known that oxidant stress increases endothelial permeability and promotes leukocyte adhesion, which are coupled with alterations in endothelial signal transduction and redox regulation of transcription factors such as activator protein-1 and nuclear factor-κB [33]. These oxidative stress-induced changes may cause intercellular gap formation, cell shape change and actin filament reorganization, which are implicated in impairment of cell contraction, cell-cell adhesion and consequently impairment of the intercellular junction, resulting in increase in paracellular permeability [33]. Many of these morphological features are considered as a primary determinant of increased permeability in various types of microvasculature. In this regard, reorganization

© 2009 The Authors
Journal compilation © 2009 Foundation for Cellular and Molecular Medicine/Blackwell Publishing Ltd

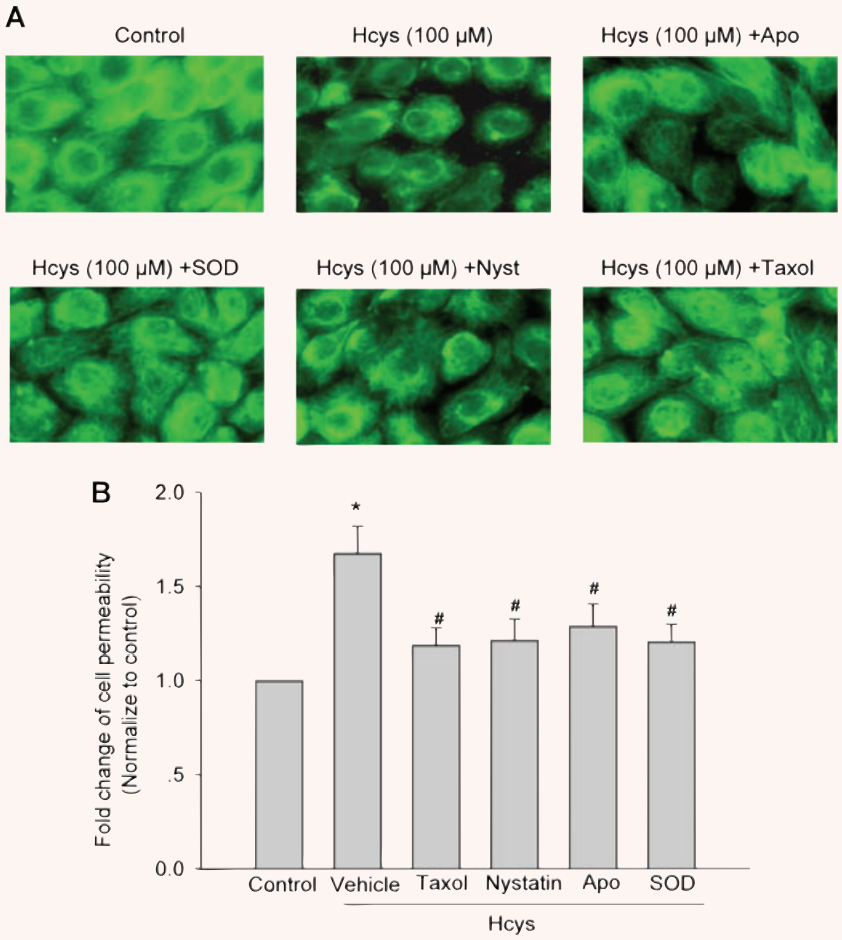

Fig. 7 Effects of microtubule network stabilizer (taxol), LR disruptors and NADPH oxidase inhibitors on Hcys-induced increase in GEC permeability. (**A**) Microscopic images showing the effect of Hcys on microtubule network structure in GECs before and after the application of these effectors. (**B**) Effects of these effectors on Hcys-induced enhancement of GEC monolayer permeability. $^{*}P < 0.05$ *versus* control; $^{\#}P < 0.05$ *versus* Hcys ($n = 5$).

of the endothelial cytoskeleton has been reported as a molecular mechanism by which endothelial cells change in their shape and intercellular gap to determine endothelial permeability [37]. Among endothelial cytoskeleton components (microfilaments of actin, microtubules and intermediate filaments), the critical role of microtubule cytoskeleton and its cross-talk with actin network have been emphasized in many studies [29, 38]. In the present study, therefore, we examined whether Hcys-stimulated LR redox signalling platforms leads to increase in the permeability in GEC monolayer by influencing the integrity of microtubule network. Since microtubules are built from a basic α/β-tubulin building block, the present study employed β-tubulin as a marker to investigate the effect of Hcys on microtubule network structure. It was found that in untreated cells, microtubules are organized into a lattice network with extensions of microtubules from the centre to the cell periphery. When GECs were treated with Hcys, collapse and shortening of microtubules with reduction of assembled microtubule were observed. These Hcys-induced alterations of microtubules could be blocked by inhibition of LR redox signalling platform formation and by scavenging $O_2^{\cdot -}$, suggesting the involvement of LR redox signalling platforms in the derangement of GEC microtubule network. This view is further supported by the results obtained in GECs treated with X/XO, an exogenous $O_2^{\cdot -}$ generating system. This exogenously produced $O_2^{\cdot -}$ also induced microtubule depolymerization and collapse which was blocked by application of SOD into the culture medium. It is concluded that Hcys-induced increase in GEC permeability is associated with oxidative stress produced from LR redox signalling platforms. It should be noted that the present study did not attempt to address how Hcys-enhanced $O_2^{\cdot -}$ production from redox signalling platforms leads to derangement of microtubule network structure in GECs. However, some previous studies have proposed that ROS induced by NADPH oxidase may activate phospholipases (*i.e.* phospholipase C, phospholipase D and phospholipase A_2), which in turn generates a multitude of cellular messengers and

© 2009 The Authors
Journal compilation © 2009 Foundation for Cellular and Molecular Medicine/Blackwell Publishing Ltd

cofactors such as Ca^{2+}, cAMP that are critical in the regulation of cytoskeleton remodelling and microtubule structures [33]. Further studies are needed to address this issue.

In summary, the present study demonstrates a novel mechanism of Hcys-induced GEC dysfunction at an early stage of hHcys. This mechanism is associated with assembling and activation of NADPH oxidase in ceramide-enriched domains in GECs, and the formation of this LR redox signalling platform may mediate the pathological actions of Hcys on the glomerular endothelium by derangement of microtubule network in these cells.

Acknowledgements

This study was supported by grants DK54927, HL075316 and HL57244 from National Institutes of Health.

References

1. **Bostom AG, Lathrop L.** Hyperhomocysteinemia in end-stage renal disease: prevalence, etiology, and potential relationship to arteriosclerotic outcomes, *Kidney Int.* 1997; 52: 10–20.
2. **Mills JL, Scott JM, Kirke PN, *et al.*** Homocysteine and neural tube defects. *J Nutr.* 1996; 126: 756S–60S.
3. **Perna AF, Ingrosso D, Satta E, *et al.*** Homocysteine metabolism in renal failure. *Curr Opin Clin Nutr Metab Care.* 2004; 7: 53–7.
4. **Suliman ME, Stenvinkel P, Barany P, *et al.*** Hyperhomocysteinemia, malnutrition, and inflammation in ESRD patients. *Semin Nephrol.* 2006; 26: 14–9.
5. **Yi F, Li PL.** Mechanisms of homocysteine-induced glomerular injury and sclerosis. *Am J Nephrol.* 2008; 28: 254–64.
6. **Li N, Chen YF, Zou AP.** Implications of hyperhomocysteinemia in glomerular sclerosis in hypertension. *Hypertension.* 2002; 39: 443–8.
7. **Yi F, Zhang AY, Janscha JL, *et al.*** Homocysteine activates NADH/NADPH oxidase through ceramide-stimulated Rac GTPase activity in rat mesangial cells. *Kidney Int.* 2004; 66: 1977–87.
8. **Yi F, Zhang AY, Li N, *et al.*** Inhibition of ceramide-redox signaling pathway blocks glomerular injury in hyperhomocysteinemic rats. *Kidney Int.* 2006; 70: 88–96.
9. **Shastry S, Ingram AJ, Scholey JW, *et al.*** Homocysteine induces mesangial cell apoptosis via activation of p38-mitogen-activated protein kinase. *Kidney Int.* 2007; 71: 304–11.
10. **Yamanaka N, Shimizu A.** Role of glomerular endothelial damage in progressive renal disease. *Kidney Blood Press Res.* 1999; 22: 13–20.
11. **Shankland SJ.** The podocyte's response to injury: role in proteinuria and glomerulosclerosis. *Kidney Int.* 2006; 69: 2131–47.
12. **Yi F, Dos Santos EA, Xia M, *et al.*** Podocyte Injury and Glomerulosclerosis in Hyperhomocysteinemic Rats. *Am J Nephrol.* 2007; 27: 262–8.
13. **Maynard SE, Min JY, Merchan J, *et al.*** Excess placental soluble fms-like tyrosine kinase 1 (sFlt1) may contribute to endothelial dysfunction, hypertension, and proteinuria in preeclampsia. *J Clin Invest.* 2003; 111: 649–58.
14. **Singh A, Satchell SC, Neal CR, *et al.*** Glomerular endothelial glycocalyx constitutes a barrier to protein permeability. *J Am Soc Nephrol.* 2007; 18: 2885–93.
15. **Bollinger CR, Teichgraber V, Gulbins E.** Ceramide-enriched membrane domains. *Biochim Biophys Acta.* 2005; 1746: 284–94.
16. **Gulbins E, Dreschers S, Wilker B, *et al.*** Ceramide, membrane rafts and infections. *J Mol Med.* 2004; 82: 357–63.
17. **Gulbins E, Li PL.** Physiological and pathophysiological aspects of ceramide. *Am J Physiol Regul Integr Comp Physiol.* 2006; 290: R11–26.
18. **Tanaka T, Miyata T, Inagi R, *et al.*** Hypoxia-induced apoptosis in cultured glomerular endothelial cells: involvement of mitochondrial pathways. *Kidney Int.* 2003; 64: 2020–32.
19. **Adler S, Eng B.** Integrin receptors and function on cultured glomerular endothelial cells,. *Kidney Int.* 1993; 44: 278–84.
20. **Fillet M, Van Heugen JC, Servais AC, *et al.*** Separation, identification and quantitation of ceramides in human cancer cells by liquid chromatography-electrospray ionization tandem mass spectrometry. *J Chromatogr A.* 2002; 949: 225–33.
21. **Zhang AY, Yi F, Jin S, *et al.*** Acid sphingomyelinase and its redox amplification in formation of lipid raft redox signaling platforms in endothelial cells. *Antioxid Redox Signal.* 2007; 9: 817–28.
22. **Jin S, Zhang Y, Yi F, *et al.*** Critical role of lipid raft redox signaling platforms in endostatin-induced coronary endothelial dysfunction. *Arterioscler Thromb Vasc Biol.* 2007; 28: 485–90.
23. **Zhang AY, Yi F, Zhang G, *et al.*** Lipid raft clustering and redox signaling platform formation in coronary arterial endothelial cells. *Hypertension.* 2006; 47: 74–80.
24. **Zhang DX, Zou AP, Li PL.** Ceramide-induced activation of NADPH oxidase and endothelial dysfunction in small coronary arteries. *Am J Physiol Heart Circ Physiol.* 2003; 284: H605–12.
25. **Siow YL, Au-Yeung KK, Woo CW, *et al.*** Homocysteine stimulates phosphorylation of NADPH oxidase p47phox and p67phox subunits in monocytes via protein kinase Cbeta activation. *Biochem J.* 2006; 398: 73–82.
26. **Zhang F, Jin S, Yi F, *et al.*** Local production of O(2)(-) by NAD(P)H oxidase in the sarcoplasmic reticulum of coronary arterial myocytes: cADPR-mediated Ca(2+) regulation. *Cell Signal.* 2007; 20: 637–44.
27. **Ying CJ, Xu JW, Ikeda K, *et al.*** Tea polyphenols regulate nicotinamide adenine dinucleotide phosphate oxidase subunit expression and ameliorate angiotensin II-induced hyperpermeability in endothelial cells. *Hypertens Res.* 2003; 26: 823–8.
28. **Hordijk PL, Anthony E, Mul FP, *et al.*** Vascular-endothelial-cadherin modulates endothelial monolayer permeability. *J Cell Sci.* 1999; 112: 1915–23.
29. **Birukova AA, Birukov KG, Adyshev D, *et al.*** Involvement of microtubules and Rho pathway in TGF-beta1-induced lung vascular barrier dysfunction. *J Cell Physiol.* 2005; 204: 934–47.
30. **McCully KS.** Hyperhomocysteinemia and arteriosclerosis: historical perspectives. *Clin Chem Lab Med.* 2005; 43: 980–6.
31. **Refsum H, Ueland PM, Nygard O, *et al.*** Homocysteine and cardiovascular disease. *Annu Rev Med.* 1998; 49: 31–62.
32. **Li PL, Zhang Y, Yi F.** Lipid raft redox signaling platforms in endothelial

© 2009 The Authors
Journal compilation © 2009 Foundation for Cellular and Molecular Medicine/Blackwell Publishing Ltd

dysfunction. *Antioxid Redox Signal.* 2007; 9: 1457–70.
33. **Lum H, Roebuck KA.** Oxidant stress and endothelial cell dysfunction. *Am J Physiol Cell Physiol.* 2001; 280: C719–41.
34. **Simionescu M.** Implications of early structural-functional changes in the endothelium for vascular disease. *Arterioscler Thromb Vasc Biol.* 2007; 27: 266–74.
35. **Seeger W, Hansen T, Rossig R, *et al.*** Hydrogen peroxide-induced increase in lung endothelial and epithelial permeability–effect of adenylate cyclase stimulation and phosphodiesterase inhibition. *Microvasc Res.* 1995; 50: 1–17.
36. **Barnard ML, Matalon S.** Mechanisms of extracellular reactive oxygen species injury to the pulmonary microvasculature. *J Appl Physiol.* 1992; 72: 1724–9.
37. **Tzima E.** Role of small GTPases in endothelial cytoskeletal dynamics and the shear stress response. *Circ Res.* 2006; 98: 176–85.
38. **Bernhard D, Csordas A, Henderson B, *et al.*** Cigarette smoke metal-catalyzed protein oxidation leads to vascular endothelial cell contraction by depolymerization of microtubules. *FASEB J.* 2005; 19: 1096–107.

© 2009 The Authors
Journal compilation © 2009 Foundation for Cellular and Molecular Medicine/Blackwell Publishing Ltd